Identification of a novel serine/threonine kinase and a novel 15-kD protein as potential mediators of the γ interferon-induced cell death

Louis P. Deiss,[1,2] Elena Feinstein,[2] Hanna Berissi, Ofer Cohen, and Adi Kimchi[3]

Department of Molecular Genetics and Virology, The Weizmann Institute of Science, Rehovot 76100, Israel

Programmed cell death is often triggered by the interaction of some cytokines with their cell surface receptors. Here, we report that γ interferon (IFN-γ) induced in HeLa cells a type of cell death that had cytological characteristics of programmed cell death. In this system we have identified two novel genes whose expression was indispensable for the execution of this type of cell death. The rescue was based on positive growth selection of cells after transfection with antisense cDNA expression libraries. The antisense RNA-mediated inactivation of the two novel genes protected the cells from the IFN-γ-induced cell death but not from the cytostatic effects of the cytokine or from a necrotic type of cell death. One of those genes (DAP-1) is expressed as a single 2.4-kb mRNA that codes for a basic, proline-rich, 15-kD protein. The second is transcribed into a single 6.3-kb mRNA and codes for a unique 160-kD calmodulin-dependent serine/threonine kinase (DAP kinase) that carries eight ankyrin repeats. The expression levels of the two DAP proteins were selectively reduced by the corresponding antisense RNAs. Altogether, it is suggested that these two novel genes are candidates for positive mediators of programmed cell death that is induced by IFN-γ.

[*Key Words*: Cell death; IFN-γ; antisense cDNA; serine/threonine kinase]

Received August 29, 1994; revised version accepted November 4, 1994.

Diffusible polypeptides such as interferons (IFNs), transforming growth factor-β (TGF-β), or tumor necrosis factor (TNF) are among the specific extracellular signals that trigger cell cycle arrest and/or cell death (Kimchi 1992). Members of these protein families interact with specific cell surface receptors and initiate putative cascades of biochemical events that suppress the proliferation of cells and/or kill them, depending on the target cell. In some cases, the cell death induced by TNF-α or TGF-β has features characteristic of the programmed type (Laster et al. 1988; Lin and Chou 1992; Oberhammer et al. 1992). Thus, some of the diffusible cytokines share common functional properties with the two membrane-bound TNF-related ligands for CD30 and Fas receptors that trigger a well-characterized process of programmed cell death (Trauth et al. 1989; Itoh et al. 1991; Smith et al. 1993; Suda et al. 1993).

In our laboratory we have recently developed a genetic approach designed for the isolation of genes that positively mediate the cytokine-triggered proliferation arrest and/or cell death (Deiss and Kimchi 1991). In principle, the method, called Technical Knock Out (TKO), is based on random inactivation of genes via the introduction of antisense cDNA expression libraries. The specific antisense-mediated inactivation of a gene along the signaling pathways is expected to confer growth advantage to cells that are continuously exposed to the cytokine and this advantage is used then as a powerful forward selection to rescue the relevant cDNA. The prerequisites for the success of the project are that the transfection will culminate in a large number of stable clones and that the vector will express high levels of the antisense mRNA transcripts and will be easily rescued from the stable transfectants. All of those features reside in an Epstein-Barr virus (EBV)-based episomal vector that we have constructed for these purposes (pTKO1; Deiss and Kimchi 1991). The first antisense cDNA clone that was isolated by this procedure, and was capable of reducing the growth sensitivity of cells to IFN-γ, corresponded to the thioredoxin gene. This proved that the project is feasible and that redox regulation of proteins is an important step in the growth-restrictive effects of IFN-γ (Deiss and Kimchi 1991).

In this work we applied the functional knockout genetic approach in a system that displays proliferation arrest followed by programmed cell death, in attempts to

[1]Present address: The George Williams Hooper Foundation, Department of Biophysics and Biochemistry, University of California, San Francisco, California 94143-0552 USA.
[2]These authors contributed equally to this work.
[3]Corresponding author.

rescue novel genes that function either as common or specific mediators of these two distinct growth-restrictive processes. We found here that 750 U/ml of recombinant IFN-γ triggered a biphasic pattern of growth responses. In the first phase the cells stopped to proliferate without loosing viability (cytostatic response phase). This was followed by a massive cell death that occurred in a nonsynchronous manner and had distinct cytological features of programmed cell death. Using the antisense knockout approach, we rescued two novel genes whose inactivation protected the cells from this type of cell death. Yet, the genetically manipulated cells remained susceptible to the cytostatic effects of IFN-γ and were not protected from a necrotic type of cell death. The cloning of the corresponding cDNAs, the deduced amino acid structure, and expression studies of the two novel proteins are described in this report.

Results

Rescue of antisense cDNAs that reduce the susceptibility of cells to IFN-γ

HeLa cells were transfected with the antisense cDNA library and selected with both hygromycin B (200 μg/ml) and IFN-γ (750 U/ml). After 28 days the cells that survived in the presence of IFN-γ were pooled, the episomal DNA was extracted, and 13 rescued pTKO-1 plasmids were analyzed further as detailed in Table 1. The cDNA inserts carried by the plasmids were classified by cross-hybridization on Southern blots into six nonoverlapping groups comprising of multiple members (groups 1 and 2) or single members (groups 3–6) (Table 1). The size of the cDNA inserts ranged between 300 and 800 bp. The cDNA inserts were then sequenced. Nucleotide sequences corresponding to groups 2–6 appeared to be novel. The four cDNA clones in group 1 were identified as fragments of human thioredoxin cDNA. Radioactively labeled PCR-amplified cDNA inserts of representative plasmids from each group were then used as probes to measure the mRNA expression on Northern blots. Each probe recognized a unique mRNA transcript in HeLa cells (Table 1).

Table 1. *Initial characterization of antisense cDNA clones rescued from HeLa cells that survived in the presence of IFN-γ treatment*

Antisense cDNA	Length of cDNA fragment (bp)	Size of mRNA (kb)	Identity
1. 241, 248, 251, 252	~350	0.7	thioredoxin
2. 230, 254, 255, 264, 258	320	2.4	novel
3. 259	252	1.7	novel
4. 253	~300	4.5	novel
5. 256	367	6.3	novel
6. 260	~800	4.0	novel

DNA inserts from the pTKO1 plasmids that cross-hybridized with each other on Southern blots were classified within the same group. The size of the antisense cDNA insert from each one of the rescued pTKO1 constructs was determined by agarose gel fractionation of the inserts (marked by ~) or by the final sequencing. The sizes of mRNAs were measured by Northern blot analysis of total RNA (20 μg) from HeLa cells using the PCR-amplified cDNA inserts of rescued plasmids as labeled probes. The identity was determined following the sequencing of each antisense of cDNA fragment and searching the nucleic acid data base.

Each of the 13 rescued pTKO1 constructs was then transfected (in duplicates) into HeLa cells to generate stable polyclonal cell populations expressing the individual antisense cDNAs. These transfectants were examined daily under phase microscope for their susceptibility to the antiproliferative and the cell-killing effects of IFN-γ. The pattern of their sensitivity to the cytokine was compared with that of two control polyclonal cell populations (designated DHFR-t1 and t2) that were transfected in parallel with a control vector—pTKO1–DHFR (Deiss and Kimchi 1991). It was found that each of the 13 rescued pTKO1 plasmids reduced the susceptibility of cells to IFN-γ and that two major types of resistant phenotypes were generated. In this work we focused on one of these phenotypes, conferred by the expression of antisense cDNAs from groups 2 and 5. This phenotype displayed reduced susceptibility to the IFN-γ-induced cell death but still remained sensitive to the cytostatic effects of the cytokine (see below).

Antisense cDNAs from groups 2 and 5 protect cells from IFN-γ-induced programmed cell death but not from growth arrest or a necrotic type of cell death

The microscopic examination of parental and control DHFR-transfected HeLa cells revealed that 750 U/ml of IFN-γ triggered a biphasic pattern of responses. The cells stopped proliferating during the first 4 days of IFN-γ treatment but still remained viable (in trypan-blue exclusion tests). They displayed a flattened morphology characteristic of the cytostatic responses to IFN-γ [Fig. 1A(b)]. The reduction in the proliferation rate during this period was also measured by a sharp decline (by >90%) in the thymidine uptake into DNA (not shown). This type of IFN-γ-induced proliferation arrest was then followed by massive cell death that occurred in a nonsynchronous fashion over a period of an additional 10 days. The cells gradually reduced their size, rounded up, and detached from the plates [(Fig. 1A(d)]. The staining of DNA with DAPI after detachment of cells from the substratum revealed gross changes in the nuclear morphology characteristic of programmed cell death. This included nuclear pyknosis, chromatin condensation, sometimes detected preferentially at the nuclear periphery, and chromatin segmentation [Fig. 1B(b)]. Transmission electron micrographs of the IFN-γ-treated cells prior to their detachment revealed other morphological changes including the disappearance of surface mi-

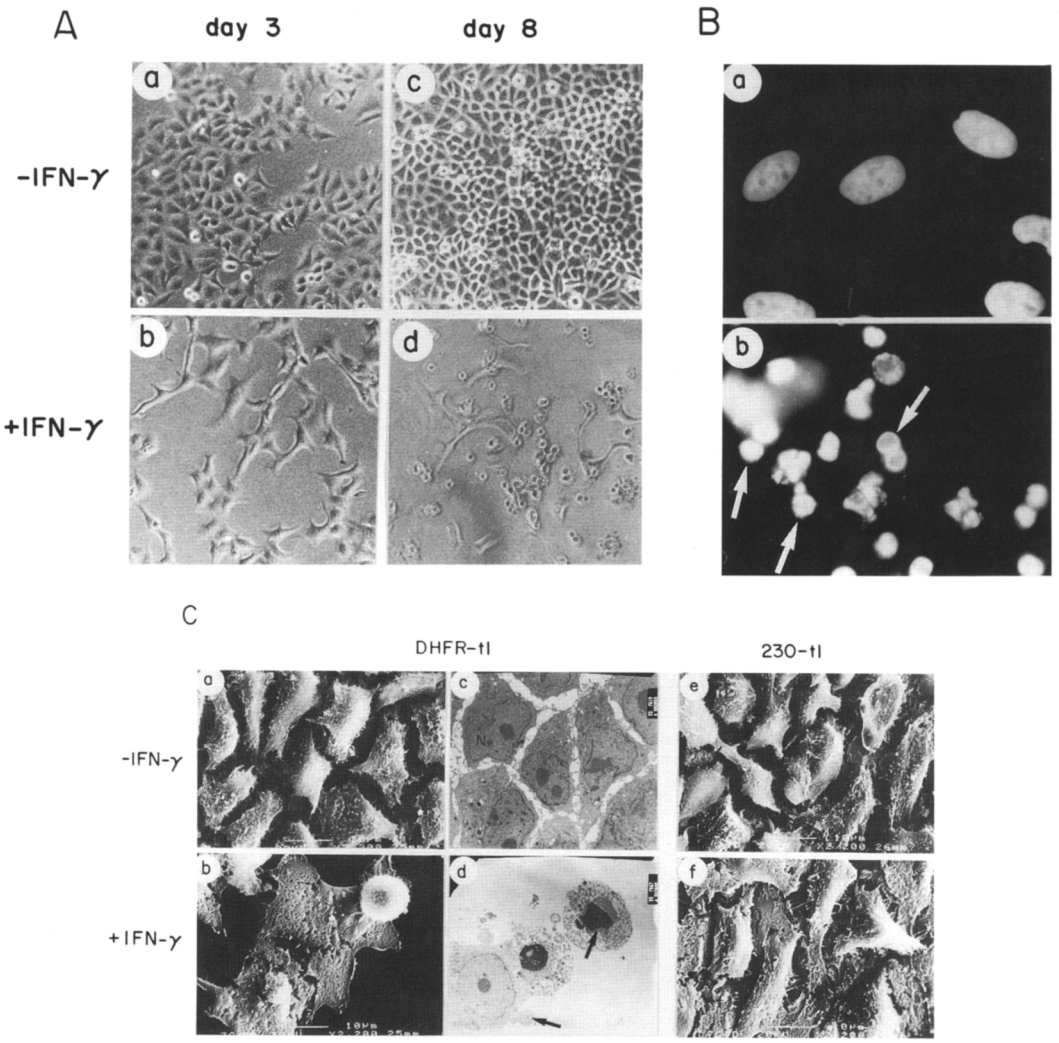

Figure 1. Morphological features of the cytostatic and cytotoxic responses to IFN-γ in HeLa cells. All cultures were seeded at an initial density of 10,000 cells/cm^2. (*A*) Light microscopy of HeLa cells transfected with pTKO1–DHFR construct (DHFR-t1 cells) on days 3 and 8 of culturing in the absence (*a,c*) or presence (*b,d*) of IFN-γ (750 U/ml). (Magnification, 260×). Note the absence of refractile mitotic cells during the cytostatic phase of responses to IFN-γ (*b*) and the appearance of round cells that were detached from the substratum during the killing phase (*d*). (*B*) Staining of DNA with DAPI. (*a*) DHFR-t1 untreated cells removed by trypsinization and mounted on glass slides; (*b*) detached DHFR-t1 cells collected 7 days after IFN-γ treatment. Nuclei with condensed or fragmented chromatin are indicated by arrows. (Magnification, 650×). (*C*) Scanning and transmission electron micrographs. DHFR-t1 HeLa cell populations (*a–d*)) and 230-t1 antisense transfected cells (*e,f*) were cultured either in the absence (*a,c,e*) or presence (*b,d,f*) of IFN-γ (750 U/ml). (*a,b,e,f*) Scanning electron micrographs were taken after 7 days using GSM 6400 SEM (Jeol). Bars, 10 μm. (Magnification, 1430× in all four samples). (*c,d*) Transmission electron micrographs taken after 7 days using a Philips 410 at a magnification of 1820×. The condensed nuclei and surface blebs are indicated by arrows.

crovilli, surface blebbing, budding off cytoplasmic projections, and cytoplasmic disintegration, in addition to the nuclear pyknosis and chromatin condensation [details shown in Fig. 1C(d)]. The antisense RNA expression from pTKO-1 plasmids of groups 2 and 5 reduced the susceptibility of the cells to the killing effects of IFN-γ: More cells survived on the plates, and the above-mentioned death-associated morphological changes appeared at much lower frequency [compare the scanning electron micrographs of the IFN-γ-treated DHFR-transfected cells in Fig. 1C(b) to the IFN-γ-treated 230-t1 cells in Fig. 1C(f)].

A neutral red uptake assay was then performed to determine more accurately, on a quantitative basis, both the typical biphasic responses of control cultures to IFN-γ and the reduced susceptibility of the antisense expressing cultures to the IFN-γ-induced cell death. The two DHFR-transfected HeLa cell populations (t1, t2) served as the control cultures in this assay, and the antisense cDNA transfected cells examined were 230-t1,

255-t1 (group 2) (Fig. 2A) and 256-t1, 256-t2 (group 5) (Fig. 2B). In the absence of IFN-γ, all of the transfected HeLa cells behaved the same and displayed practically identical growth curves suggesting that the antisense RNA expression had no effects on the normal growth of cells. Another feature that was not changed by the antisense RNA expression was the extent of the cytostatic responses to IFN-γ. As shown in Figure 2, A and B, IFN-γ has similarly reduced the proliferation rate of all the transfected cultures and they all displayed the same extent of reduction in the neutral red dye uptake during the first 4 days (before cell death starts to be microscopically evident). After 4 days of treatment the picture changed drastically. Whereas almost all control cells died during the following days of IFN-γ treatment leading to minimal values of the neutral red dye uptake on day 14, a significant fraction of cells that expressed antisense RNA survived in the presence of IFN-γ, as reflected by the sustained values of the dye uptake. The resistance to the IFN-γ-induced cell killing was very similar in all four

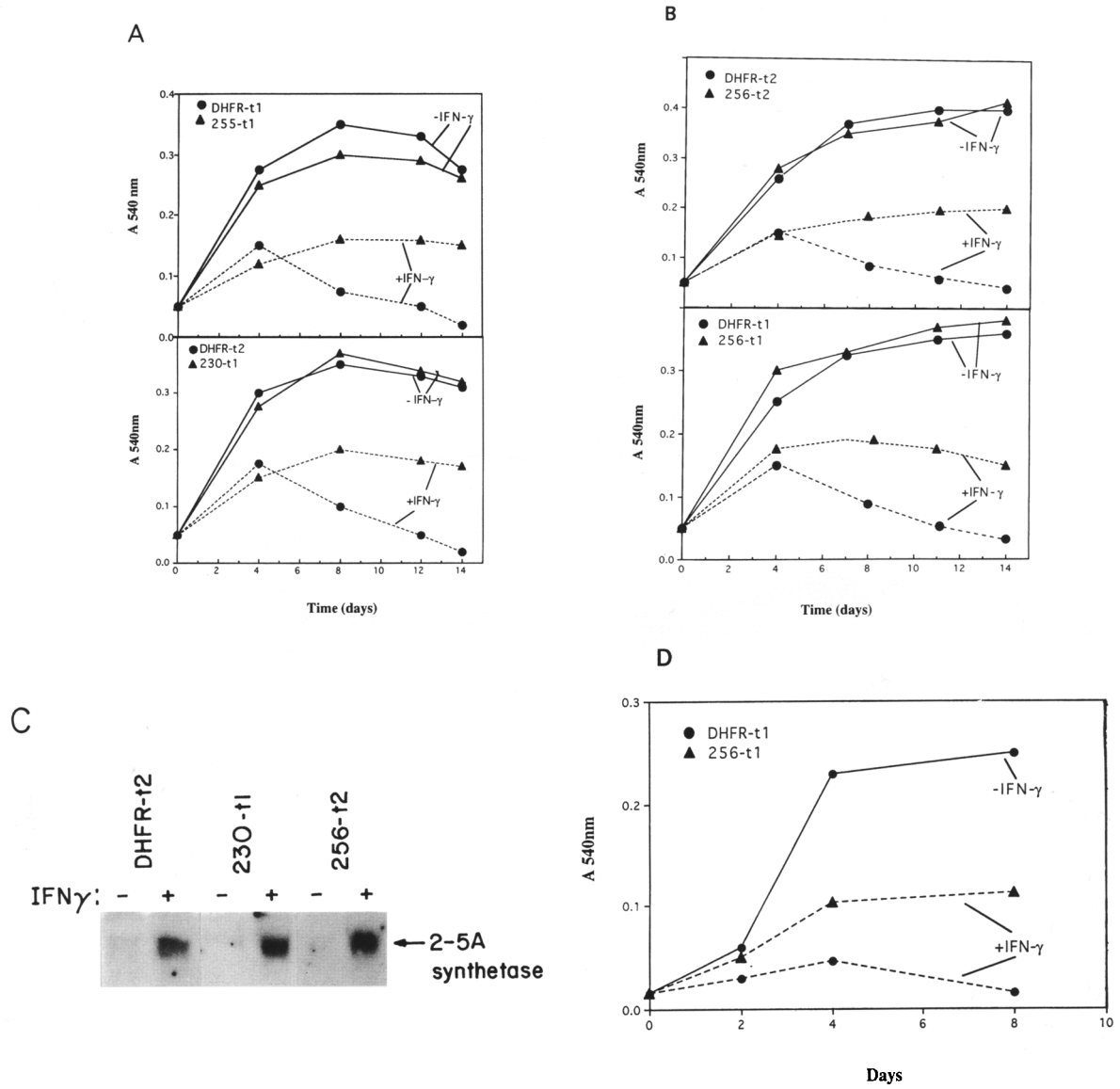

Figure 2. Antisense RNA expression from plasmids of groups 2 and 5 reduces the susceptibility of HeLa cells to the killing effects of IFN-γ. (*A,B,D*) Neutral red dye uptake. The different transfected HeLa cell populations were cultivated in 96-well microtiter plates at an initial number of 15,000 cells/well. They were then treated with IFN-γ: 750 U/ml in *A* and *B*; 5000 U/ml in *D* (dashed lines). The rest of the wells were left untreated (solid lines). All of the cells were maintained continuously in hygromicin B. Viable cells were stained with neutral red (Sigma), and the dye uptake was measured at λ = 540 nm using an automated Micro-Elisa auto-reader. (●) DHFR-t1 and DHFR-t2 control cells; (▲) Antisense transfected cells corresponding to group 2 (*A*) or group 5 (*B,D*). Each point is the average of a quadruplicate determination with a S.D. that ranged between 2% and 5%. (*C*) Northern blot analysis of 2-5A synthetase gene induction. The indicated HeLa cell transfectants were incubated for 24 hr in the presence (+) or absence (−) of IFN-γ (750 U/ml). Twenty micrograms of total RNA was analyzed. The cDNA of the 2-5A synthetase was used as probe.

tested cultures that expressed the two different antisense RNAs (Fig. 2A,B). These data indicate that expression of antisense RNA from groups 2 and 5 protects the HeLa cells exclusively from the IFN-γ-induced cell death and not from its cytostatic action. It is noteworthy that the antisense RNA expression did not affect the early biochemical steps in the signaling of IFN-γ as deduced from the normal induction of 2-5A synthetase mRNA in these transfected cells upon IFN-γ treatment (Fig. 2C).

To test whether the time kinetics of cell death could be accelerated, the HeLa cells were exposed to increasing concentrations of IFN-γ. Upon addition of 5000 U/ml of IFN-γ, cell death was already prominent in the cultures on day 2 and reached almost maximal values (15% viable cells) on day 4 (Fig. 2D). The dying cells had the microscopic characteristics of programmed cell death as described above. Under these accelerated time kinetics, the protection by the antisense RNA remained prominent, as quantitated by the neutral red uptake assay (Fig. 2D). This line of experiments supports the notion that the process of cell death that develops in this system is an integral part of the IFN-γ effects on cells; therefore, the genes that were inactivated by the antisense RNA expression may act as mediators of the IFN-γ -triggered programmed cell death.

It became interesting at this stage to check whether antisense RNA expression can also protect the HeLa cells from a necrotic type of cell death. For this, the combinatorial effect of TNFα and cycloheximide (CHX) was examined in the various HeLa cell populations. Unlike the effect of IFN-γ, the cell death that was induced by TNFα + CHX in HeLa cells was very rapid (50% killing after 3 hr) and displayed typical features of necrosis such as swelling of the cells before their lysis. As shown in Table 2, although the antisense RNA expression from groups 2 and 5 protected the cells from the IFN-γ-induced cell killing, there was no protection from the TNFα-induced necrotic cell death. All of the examined HeLa cell transfectants were killed by the TNF + CHX combination with similar time kinetics and at the same efficiency. Northern blot analysis demonstrated that the levels of the antisense mRNA transcripts in 256-t1 cells were not reduced by the TNF + CHX treatment at 5 hr (not shown), thus excluding the possibility that loss of the antisense RNA expression caused by the treatment may be the reason for lack of protective effects from the necrotic cell death. This suggests further a certain specificity of the protective mechanisms regarding the type of cell killing.

Cloning of the DAP-1 cDNA, deduced amino acid structure, and expression studies

The 320-bp cDNA fragment from construct 230 (group 2) hybridized on Northerns blots to a single endogenous 2.4-kb mRNA transcript in HeLa cells (Fig. 3A). In stable transfectants carrying antisense constructs 230 or 255 (group 2) but not 260 and 259 (groups 6 and 3, respectively), a composite antisense 1.1-kb transcript was also detected by this probe (Fig. 3A). It consisted of 320 bases of the cDNA insert and 800 bases of sequences derived from the expression cassette (Deiss and Kimchi 1991). The antisense orientation of fragment 230 in the pTKO1 vector was reconfirmed upon sequencing of the sense cDNA clone (see below). The amount of the antisense RNA expressed from clones 230 and 255 (group 2) in growing HeLa cells exceeded the sense mRNA levels by three- to sixfold (Fig. 3A,B). Because of the presence of IFN-stimulated response element in the pTKO1 vector (Deiss and Kimchi 1991), after IFN-γ treatment the levels of antisense mRNA expression were elevated further leading to 15-fold excess of antisense over sense transcripts (Fig. 3B). The endogenous 2.4-kb mRNA appeared as a single transcript also when the full-length cDNA was used as a probe and its levels were not modulated by IFN-γ (Fig. 3B).

An HL-60 cDNA library constructed in λgt10 vector was screened with the cDNA insert of pTKO1-230 after varifying that these cells express the 2.4-kb mRNA. Two independent clones, λ1 and λ2, almost completely overlapping and carrying cDNA inserts of ~2.3 kb, were analyzed. The λ1 cDNA clone encompasses the 5′-untranslated region, short coding region(s), and a relatively long 3′-untranslated region that constitutes >60% of the cDNA clone (Fig. 4A). This cDNA is 2232 bp long and contains a potential polyadenylation signal (ATTAAA) at its 3′ end. The open reading frame (ORF) is very short starting from the initiation codon at nucleotide positions 160–162 and ending at termination codon TGA at positions 466–468 (Fig. 4B). This ORF is preceded by an ex-

Table 2. *Expression of antisense RNA (from groups 2 and 5) protects from IFN-γ-induced programmed cell death but not from TNF-induced necrotic cell death*

		DHFR-t1	DHFR-t2	230-t1	255-t1	256-t1
				A = 540 nm		
14 days	No treatment	0.396	0.345	0.385	0.324	0.336
	IFN-γ	0.026	0.017	0.136	0.158	0.159
5 hr	No treatment	N.D	0.148	0.130	N.D	0.140
	TNF-α + CHX	N.D	0.053	0.026	N.D	0.022
20 hr	No treatment	0.211	0.248	0.223	0.173	0.190
	TNF-α + CHX	0.002	0.001	0.003	0.0015	0.002

Each treatment was done in quadruplicate, and the average values of dye uptake, measured by OD at λ = 540 nm, is presented at the indicated time intervals. The S.D. was between 2% and 4%. (N.D.) Not done.

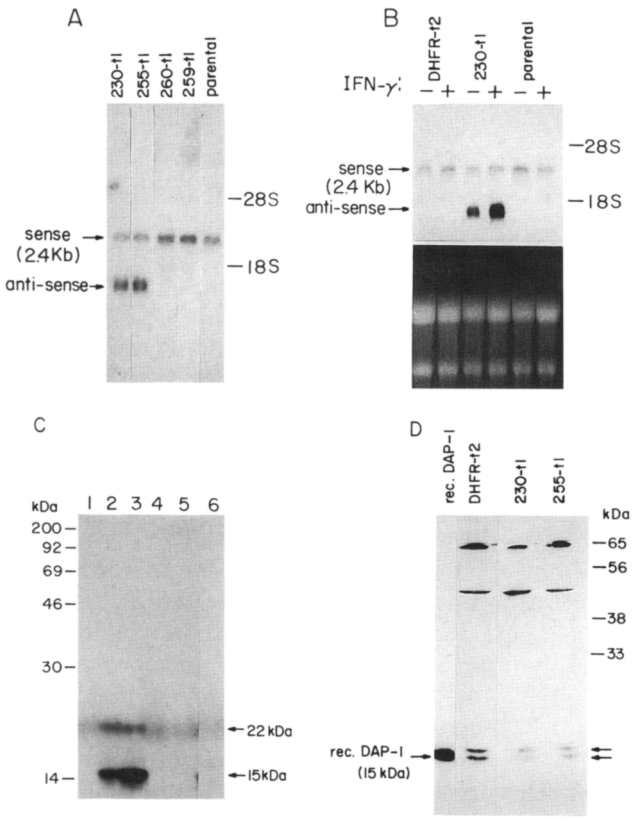

Figure 3. RNA and protein expression of DAP-1 gene. (*A*) Total RNA was prepared from HeLa cells either before (parental) or after transfection with pTKO1 construct 230 or 255 (group 2), 260 (group 6), and 259 (group 3) designated 230-t1, 255-t1, 260-t1 and 259-t1, respectively. Twenty micrograms of RNA was processed on Northern blots, and DNA fragment 230 was used as a probe. The arrows point to positions of sense and antisense RNAs. (*B*) RNA was extracted from the indicated HeLa cells that were grown for 4 days in the absence (−) or presence (+) of IFN-γ (750 U/ml). The Northern blot containing 20 μg of RNA samples was hybridized with the cDNA insert of phage λ1. Ethidium bromide staining of the RNA samples is shown. (*C*) In vitro translation of RNA (0.5 μg) transcribed from λ1 cDNA (lane *2*) and from subclones p6, p4, p5, and p8 (lanes 3–6, respectively). (Lane *1*) Background obtained in the absence of RNA administration to the reticulocyte lysates. The labeled proteins were fractionated on 12% SDS–polyacrylamide gels. The positions of the radioactive molecular mass markers (Amersham) are marked. The two translated proteins, major 15-kD and minor 22-kD proteins, are indicated by arrows. (*D*) Immunoblot analysis of recombinant and cellular 15-kD DAP-1. Bacterially produced DAP-1 (300ng) and the indicated HeLa cell extracts (350 μg) were fractionated on SDS–polyacrylamide gels (12%), blotted to nitrocellulose, and reacted with affinity-purified antibodies generated against 15-kD DAP-1. The cells were treated with IFN-γ (750 U/ml) for 4 days before extraction. The two arrows point to the position of cellular DAP-1. The antibodies also recognize two nonrelevant bands of 60 and 45 kD that are not modulated by antisense RNA expression. Quantitation of the reduction in DAP-1 was done by densitometric analysis. The calibration of the protein content in each slot was done by referring to the signals of the nonrelevant bands. The prestained protein markers (Sigma) are marked.

tremely GC-rich 5′-untranslated region and potentially codes for a protein consisting of 102 amino acids with a calculated molecular mass of 11.2 kD.

The amino acid composition predicts a basic protein (pI 10), rich in prolines (15%). The high proline content may cause some anomalies in the protein's migration on gels. Search for motifs (Motifs program; GCG Software Package) indicated that the protein contains two potential sites for casein kinase II phosphorylation at positions 3 and 36, a single potential protein kinase C phosphorylation site at position 91, and a consensus phosphorylation site of the cyclin-dependent kinases (cdks) at position 51. In addition, the protein contains the consensus sequence RGD at position 65–67, a tripeptide that in some proteins plays a role in cell adhesion (Ruoslahti and Pierschbacher 1986) and a potential SH3-binding motif, xPxPP, at position 49–53 (for review, see Cowburn, 1994). No indications for the presence of signal peptide or transmembranal domain have been found (SAPS prediction; Brendel et al. 1992). The amino acid sequence showed no significant homology to known proteins. Use of SBASE domain library (Pongor et al. 1992) revealed a stretch of amino acids at position 30–46 with significant homology to the repeated elements in the sarcoplasmic reticulum protein that are involved in Ca^{2+} binding (Hofmann et al. 1989). This new protein was named DAP-1 (death-associated protein-1).

In vitro translation assays in reticulocyte lysates established that the predicted ORF codes for a 15-kD protein. The full-length cDNA insert as well as four subclones that span different regions of the molecule (i.e., p6, p5, p8, and p4; see Fig. 4A) were transcribed and translated in cell-free systems. Among all of the tested subclones, only the 5′ 1-kb portion of the DAP-1 cDNA (p6) directed the in vitro synthesis of proteins (Fig. 3C). The major translated product migrated on gels as a 15-kD protein. Mutation at the ATG codon at position 160–162 (ATG → GGC) completely eliminated the synthesis of the 15-kD protein, thus confirming the position of the start point of this protein (data not shown). In addition to the 15-kD protein product, a second protein of 22 kD was also translated at lower efficiency from λ1 and the p6 cDNAs (Fig. 3C). Its translation was not influenced by the elimination of the ATG codon at position 160, but the protein was reduced to a size of 16 and 18 kD upon cleavage of the p6 subclone with *Dra*I and *Bst*YI restriction endonucleases, respectively (not shown; for restriction map, see Fig. 4A). These criteria fit another potential ORF, which is detected in the nucleotide sequence in a different phase with respect to the first ORF (Fig. 4A). It starts at the ATG codon (position 287–289) and ends at termination codon TGA (positions 816–818). It has the potential to code for a protein consisting of 176 amino acids with calculated molecular mass of 19.9 kD and no significant homology to known proteins. It will be of interest to test whether this second ORF also can be utilized by intact cells.

To analyze the expression of the major DAP-1 in cells, polyclonal antibodies were made to the bacterially produced 15-kD protein. The affinity-purified antibodies

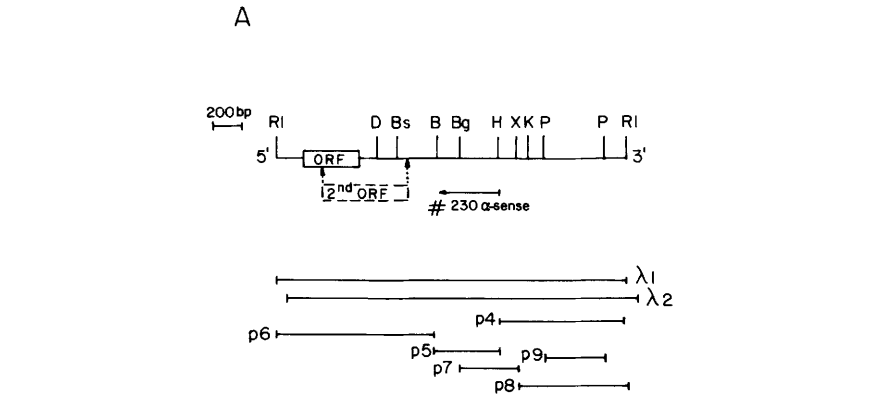

B

```
CGTGGCACTCACCCGGCTCGCGCGGCCCCGGCCGCCCACGCCGCGCGTCGTTCTCCCGCCCGCTCGCTCCCCGGCGCTCACACCTGAGCT      90

                                                                  M  S  S  P  P  E  G      7
CACTCGCGCACGCCCGCCCGGCCCGAGAACCGCGCCGCCGCCTCGGCCCCGCGGAAGCCCCGCCGCGCCATGTCTTCGCCTCCCGAAGGG    180

K  L  E  T  K  A  G  H  P  P  A  V  K  A  G  G  M  R  I  V  Q  K  H  P  H  T  G  D  T  K     37
AAACTAGAGACTAAAGCTGGACACCCGCCCGCCGTGAAAGCTGGTGGAATGCGAATTGTGCAGAAACACCCACATACAGGAGACACCAAA    270

E  E  K  D  K  D  D  Q  E  W  E  S  P  S  P  P  K  P  T  V  F  I  S  G  V  I  A  R  G  D     67
GAAGAGAAAGACAAGGATGACCAGGAATGGGAAAGCCCCAGTCCACCTAAACCCACTGTGTTCATCTCTGGGGTCATCGCCCGGGGTGAC    360

K  D  F  P  P  A  A  A  Q  V  A  H  Q  K  P  H  A  S  M  D  K  H  P  S  P  R  T  Q  H  I     97
AAAGATTTCCCCCCCGGCGGCTGCGCAGGTGGCTCACCAGAAGCCGCATGCCTCCATGGACAAGCATCCTTCCCCAAGAACCCAGCACATC    450

Q  Q  P  R  K  *                                                                            102
CAGCAGCCACGCAAGTGAGCCTGGAGTCCACCAGCCTGCCCCATGGCCCCGGCTCTGCTGCACTTGGTATTTCCCTGACAGAGAGAACCA    540
GCAGTTTCGCCCAAATCCTACTCTGCTGGGAAATCTAAGGCAAAACCAAGTGCTCTGTCCTTTGCCTTACATTTCCATATTTAAAACTAG    630
AAACAGCTTCAGCCCAAACCTTGTTTATGGGGAGTCTGGTTGGATGTCATTTGAGGATCATTGTGCCCCTAGAGGTGCCATTAGCAGAAT    720
TTGCCAAGATCCGAGAAAAATTTTAGCTTTAGTTCTATTTCAGCAGTCACCTGACGTCCTTGTCTATGGTCTTAAAAACAAGAAGGCACA    810
CATTTGAGAAGATGAGATTAAGGTTAGGAGAAAACCTCAGTCATTGCATGCTTTTTAGTATGGGCCAATAAAATCTCAACACCTGTGGGA    900
GAGTAAGAACTAAGGGAATGAGTTTGGGCGCCCCCTCATAAAGGACCTTAGAGGCAGGGAACAGCAATGCCAAATTTCCCTCTCTCGTGA    990
GATGGGGGATCCTGTGCAGGCTGATGAGGCACCCATGAGAAAAGCCGAAAAAGCATGCATCTTAGAAATAGCCCCTCAATTCCAGGAGTC   1080
AACATGCCAAAGAATGAGGCTGGAGACAGGTAGCTCCGAGGGAGGACTTCTGGCATGAGATCTCGGCACGGCAAGCCCAGCATCGCCTCA   1170
GCCCAGACAGGCTCCACCAGGAGATCAAGCAAGGGCTGCCTTTCAGGAGTCACCTCCTGAGCCACTTCAGAGTTCTGGAAGTGACCACGG   1260
ACCAGGGTGGAGGAATAGACTTCTAGTTCATTCTGGGACACTTGAGCCAGAGAGTTGAAAGCTTGGAAAGACCAGATAAGAAACCTGCCC   1350
TTTGTCTCCCTAGGGACATGAGACACCACATTCCATTTGTGCTAGAAAAACCTATCCACTGATGAGTCTAACTGTTCCAAACGCCTCCCA   1440
CCTGGTGTGCACAGCTGCCTGGGTCCATTGTCACTTGGGTGCATCAGGTTGTCCTCCGATTTTTAGATGAGTTTCCTGTCTAGAGATGTC   1530
CTAGTCTGCTCACTGGCTGGTGGCAGTAGGGTACCCTGCGTCCTCGAAAAGCCAGAGGGTTCACCTAGTCAGACGAAACTCCAGAACAGT   1620
GCTTGTGGAGGGCCTGACTGTCCTGCTCACCCACAGCCGATCTGCTGCAGGTCAGCAACTGTGTCGTGAGCAGCTGCCAACCACCAGCCT   1710
TTCTGGTGCTGTTCTCCAGTTCACGTCTGCCAGCTGGTGAGGGCAGAGGCAGACCTGGTCAGACCCAGCGCCCCTCCTCCCTGAGGGAGC   1800
ATGGCACAGCCTCACACTTGAAAGACGGTGTTTGGTTTCCCATCTAATCAACTTAAGGGAAGCCGGCATGTACCCTTCAAGGCCCTGTCA   1890
CCACCTATTTTCCTGATCAGTTGGTATAAACTGAGGGTGGCTTTTAGAGACCCAGACTTGGTTGGCAGCGCTGCCATGGAACACCCCAGC   1980
AAGCACCTCCCAGCCTGCCTTTCGGAGCAGCACCCAGGAGGGGATGCCGCGCTCCAGCAACACCAGGTCAGGCCTGTGCAGACCCCTGCC   2070
CTGCCGCTGCAGAAATCCAGAAGCATCCTTAATGCTTCTCAGTCTTCAGCCAGAGGGAGGGCTGTTATTTCCAGAGGTGCGCTTTTTATG   2160
TACTTTTAGCTAGATGTGGCATGCATCTGTGAGCTTTAGATCATTAAATCCAAAATGTTTGCCTAAATGAGG                      2232
```

Figure 4. Nucleotide sequence and predicted amino acid pattern of DAP-1 cDNA. (*A*) Schematic representation and restriction map of DAP-1 cDNA. The open box (solid line) represents the major ORF. A potential second ORF is boxed with broken lines. The position of the antisense 230 cDNA fragment is shown. λ1 and λ2 represent the λgt10 phage inserts that were used for cDNA sequencing. p4, p6, p5, p9, p7, and p8 are subclones derived from the λ1 cDNA insert used for the sequencing and for in vitro translations. The cleavage sites for major restriction enzymes are shown. (RI) *Eco*RI; (D) *Dra*I; (Bs) *Bst*YI; (B) *Bam*HI; (Bg) *Bgl*II; (H) *Hin*dIII; (X) *Xho*I; (P) *Pst*I. (*B*) Nucleotide sequence of the DAP-1 cDNA and its deduced amino acid structure. Initiation (ATG) and stop (TGA) codons are boxed. A potential polyadenylation signal is underlined. The RGD and SH3 binding motifs are marked by brackets.

recognized on immunoblots two closely migrating proteins in extracts of HeLa cells; the lower band comigrated on gels with the bacterially produced 15-kD DAP-1 (Fig. 3D). The slow migrating form may represent a post-translationally modified version of the protein. In HeLa cell transfectants, 230-t1 and 255-t1, expressing the elevated levels of antisense RNA detected after exposure to IFN-γ (15:1 ratio of antisense/sense RNA), the DAP-1 protein levels were reduced by 75% and 78%, respectively, as compared with the levels in the control DHFR-tranfected cultures (Fig. 3D). The antibodies also reacted with two other nonrelevant proteins of 60 and 45 kD, which were used as an intrinsic reference for calculating the extent of selective reduction in DAP-1 by antisense RNA expression. Also signals that were generated in the same immunoblot after reaction with anti-vinculin antibodies were used as a constitutive reference (not shown).

Cloning of the DAP kinase and deduced amino acid structure of the encoded protein

Expression studies indicated that the double-stranded cDNA fragment 256 (367 bp in size) hybridized on Northern blots to an endogenous 6.3-kb mRNA transcript. In the 256-t1 and 256-t2-transfected cells it also hybridized to a composite antisense 1.2-kb RNA transcipt (Fig. 5A). The antisense orientation of fragment 256 in the pTKO1 vector was confirmed upon sequencing of the sense cDNA clone (Fig. 6A). The amount of the antisense RNA expressed from pTKO-1 plasmid 256 in untreated HeLa cells exceeded the sense mRNA levels by >100-fold. Treatment with IFN-γ further increased the antisense RNA levels because of the presence of an IFN-stimulated response element in the episomal vector. The same single 6.3-kb mRNA transcript was detected in HeLa cells (parental and transfectants) when the full-length cDNA was used as a probe on Northern blots (Fig. 5B). The steady-state levels of the 6.3-kb sense mRNA transcript were increased by three- and sevenfold at 24 and 72 hr of treatment with IFN-γ, respectively (Fig. 5C), suggesting a link between cytokine signaling and the expression of this gene.

The cDNA insert from pTKO1-256 was used to screen a K562 λgt10 cDNA library after verification that the gene is expressed in K562 cells (Fig. 5B). Two λgt10 clones, λ29 and λ32, were chosen for sequencing (Fig. 6A). The resulting composite sequence of both cDNAs

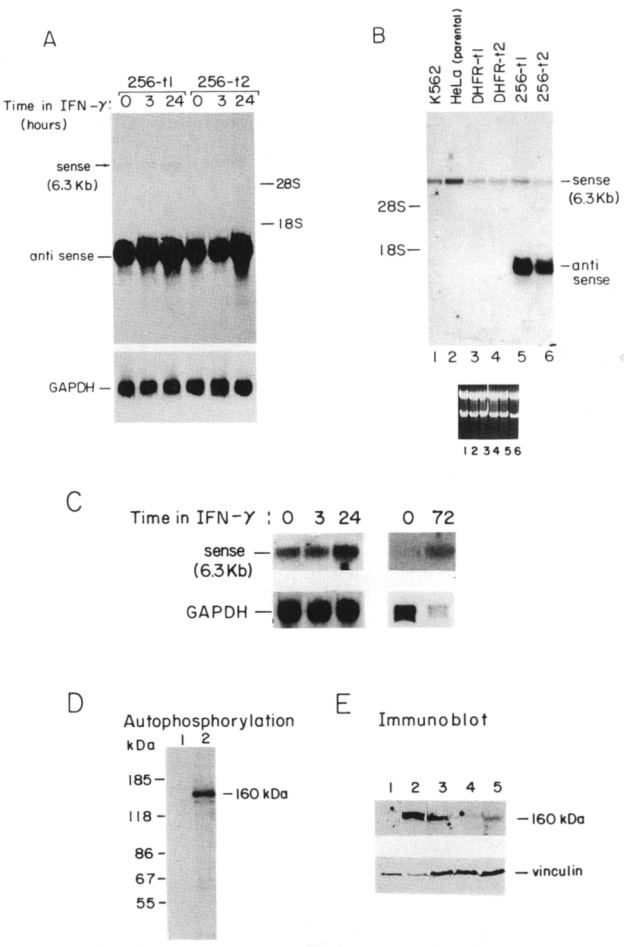

Figure 5. RNA and protein expression of DAP kinase. (*A*) Total RNA was prepared from 256-t1 and 256-t2 HeLa cell transfectants either before (0 hr) or at 3 and 24 hr after treatment with IFN-γ (750 U/ml), and 20-μg samples were processed on Northern blots. Fragment 256 was used as a probe. The positions of the sense and antisense mRNAs are indicated. The GAPDH mRNA levels were used for the calibration of the RNA amounts in each slot. (*B*) The blot consists of total RNA (20 μg) from K562 cells, parental HeLa cells, the two DHFR-transfected HeLa cell populations and the two HeLa cell populations that were transfected with pTKO1-256. The blot was hybridized with the cDNA insert of λ29. Ethidium bromide staining of the RNA samples is shown. (*C*) Total RNA prepared from DHFR-transfected HeLa cells either before (0 hr) or at 3, 24, and 72 hr after treatment with IFN-γ (750 U/ml). The blot was hybridized with the cDNA insert of λ29. (*D*) In vitro phosphorylation assay. Cell lysates were prepared from COS-7 cells either before (lane *1*) or after transfection with the PECE–FLAG expression vector that carries the coding region of the λ29 cDNA (lane *2*). Samples of 400 μg were immunoprecipitated with anti-FLAG (M2) monoclonal antibodies (IBI) and subjected to phosphorylation assays as detailed in Materials and methods. (*E*) Immunoblot analysis of recombinant and cellular DAP kinase protein. COS-7 cells were transiently transfected with the PECE–FLAG–DAP kinase expression vector. Samples of cell lysates—100 μg from COS-7 cells and 400 μg from HeLa cells—were fractionated on SDS–polyacrylamide gels (7.5%), immunoblotted, and reacted with affinity-purified polyclonal antibodies raised against the amino-terminal DAP kinase peptide. (*Bottom*) The blot was reacted with monoclonal antibodies against vinculin (Sigma Immunochemicals). (Lane *1*) Nontransfected COS-7 cells; (lane *2*) transfected COS-7 cells; (lane *3*) DHFR-t1 cells; (lane *4*) 256-t1 cells; (lane *5*) 256-t2 cells. In lane *2* the same 160-kD protein was also detected with anti-FLAG (M2) monoclonal antibodies (IBI) (not shown).

consists of 5886 nucleotides and contains a poly(A) tail that starts at position 5872 and is preceded by each of two polyadenylation signals, AATAAA (Fig. 6B). The 3′-untranslated region also contains two ATTTA instability motifs found in the 3′-noncoding portions of short-lived mRNAs (Shaw and Kamen 1986). The mRNA contains a single long ORF that starts at position 337, ends at position 4605, and potentially codes for a protein of 1423 amino acids (Fig. 6B). The calculated molecular mass of the protein product is ~160 kD. Affinity-purified polyclonal antibodies were raised against the amino-terminal 20-amino-acid peptide of the protein. These antibodies recognized on immunoblots a recombinant 160-kD protein that was produced in COS-7 cells after transfection with a vector that expressed the entire coding region of the cDNA (Fig. 5E). In nontranfected HeLa cells these antibodies reacted with an endogenous protein of the same size. In antisense RNA-expressing cells 256-t1 and 256-t2 the steady-state levels of the 160-kD protein were, respectively, 10- and 5-fold lower than in the DHFR control cells, whereas a nonrelevant protein, vinculin, displayed similar expression levels in all HeLa cell transfectants (Fig. 5E). Thus, expression of antisense RNA from pTKO-1 plasmid 256 in HeLa cells resulted in

Figure 6. Nucleotide sequence of the DAP kinase cDNA and its deduced protein structure. (*A*) Schematic representation of the restriction map of DAP kinase cDNA. The ORF is indicated. λ29 and λ32 represent the λgt10 cDNA inserts that were used for sequencing. The cleavage sites for major restriction enzymes are shown. (A) *Ava*I; (B) *Bam*HI; (Bg) *Bgl*II; (H) *Hin*dIII; (RI) *Eco*RI. The position of the antisense fragment 256 is indicated. (*B*) Nucleotide and amino acid sequence. Initiation (ATG) and stop (TGA) codons are boxed. Upstream short ORFs are underlined with an arrow. Polyadenylation signals are simply underlined; mRNA instability signals (ATTTA) are underlined with a wavy line. Protein kinase domain, calmodulin-regulatory region, ankyrin repeats, and potential P-loop sites are indicated. The deduced amino acids structure predicts 6 N-glycosylation sites, 6 potential cAMP-dependent kinase phosphorylation sites, 28 potential casein kinase II phosphorylation sites, and 20 potential protein kinase C phosphorylation sites. DAP kinase protein contains a consensus sequence for the carboxy-terminal amidation site at position 1376 (this suggests that 47 carboxy-terminal amino acids can be cleaved from the protein). (*C*) Schematic diagram of the predicted DAP kinase protein. The hatched box indicates the calmodulin regulatory region. The numbered boxes indicate the eight ankyrin repeats. The wavy lines correspond to the two potential P-loop sites.

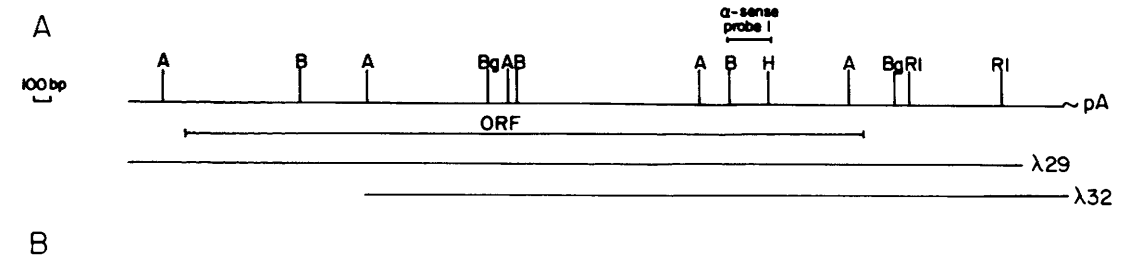

B

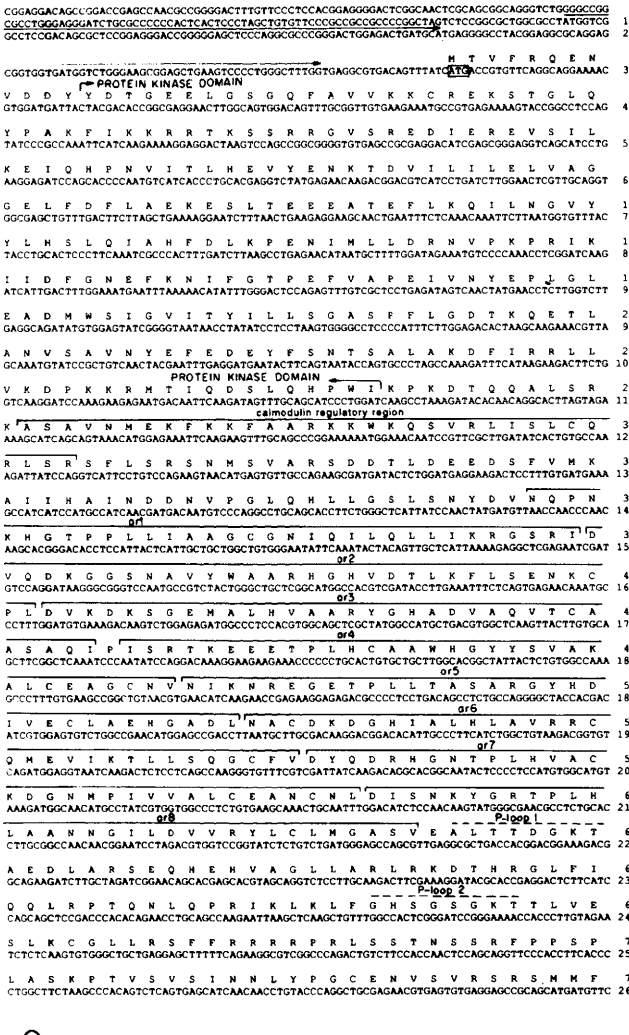

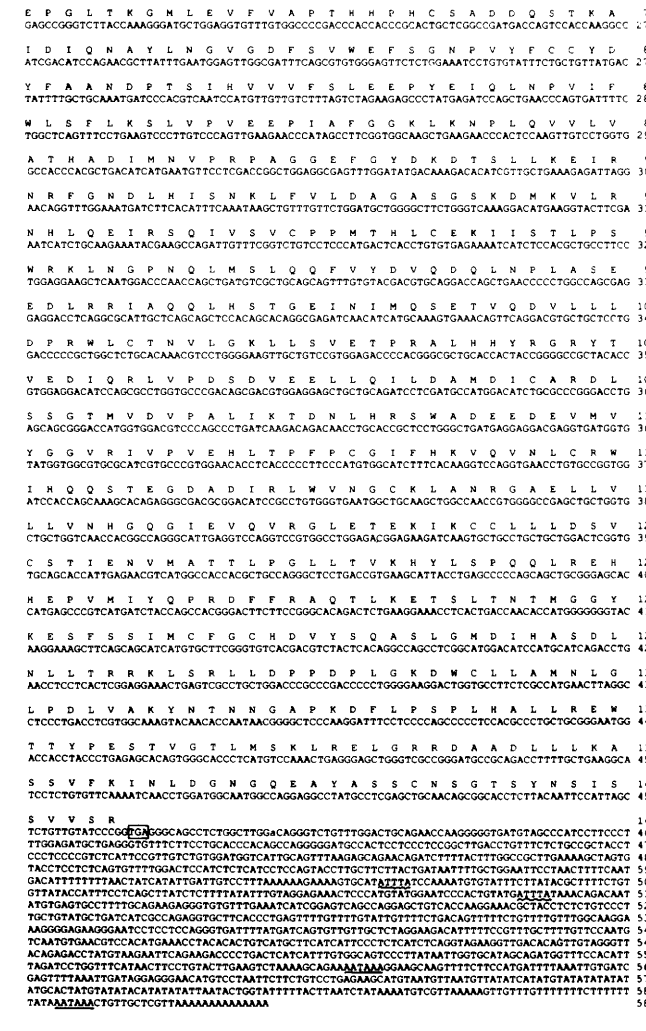

C

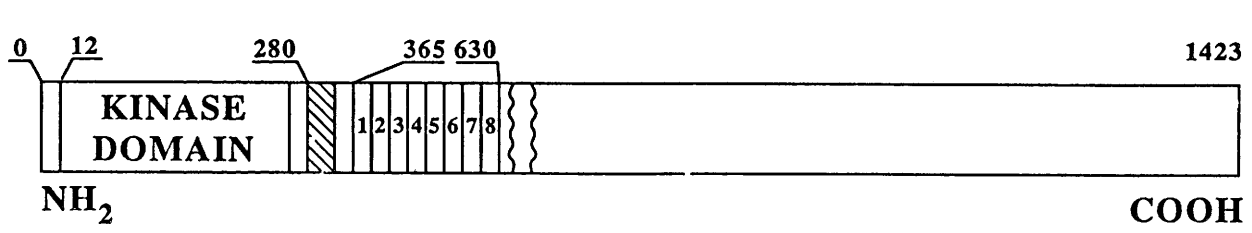

Figure 6. (*See facing page for legend.*)

a significant reduction in the amount of the corresponding protein.

We were able to define several known domains and motifs that are present in this protein. Its very amino terminus is composed of a protein kinase domain that spans 255 amino acids from position 13–267. According to its structure it is likely to be a serine/threonine type of protein kinase and has a classical composition of XI subdomains with all conserved motifs present (Figs. 6B and 7A) (Hanks and Quinn 1991). In vitro autophosphorylation assays confirmed that the protein possesses a kinase activity. FLAG-tagged recombinant 160-kD protein, produced in COS cells, was immunoprecipitated with anti-FLAG antibodies and subjected to in vitro phosphorylation assays. A single prominent ^{32}P-labeled band of 160-kD appeared upon SDS–polyacrylamide gel fractionation only in samples prepared from the transfected cultures (Fig. 5D). Substitution of the conserved lysine 42 residue in subdomain II with alanine, a point mutation that was shown to interfere with the phosphotransfer reaction in other kinases (Hanks et al. 1988), abolished the phosphorylation of this band (not shown). It is suggested that the 160-kD protein displays an intrinsic kinase activity and undergoes autophosphorylation. This novel kinase was termed DAP kinase.

The kinase domain falls into a family of calmodulin-dependent kinases (Hanks and Quinn 1991). The homology to known kinase domains that constitute this group, including the myosin light chain kinases, ranges between 34% and 49% (Fig. 7A). Three main differences distinguish the kinase domain of DAP kinase from other members of the calmodulin-dependent kinase family: (1) Subdomain II is relatively long and has a stretch of basic amino acids (KKRRTKSSRR) (Fig. 7A). (2) Subdomain III primarily resembles that of the cell cycle-dependent kinases (Fig. 7B). Interestingly, the typical sequences of the cell cycle-dependent kinases (PSTAIRE, PSSALRE, PCTAIRE, KKIALRE) are located in subdomain III. (3) Subdomain VII is extremely short and consists of only 7 amino acids. Just downstream of the kinase domain lies an additional stretch of homology that is present in almost all members of the family of calmodulin-dependent kinases (Fig. 7A) and was implicated in calmodulin-recognition and binding (Blumenthal et al. 1985; Guerriero et al. 1986; Herring et al. 1990; Olson et al. 1990; Shoemaker et al. 1990; Cruzalegui et al. 1992). Downstream of the calmodulin-recognition domain an ankyrin repeat domain (Michaely and Bennette 1992) was identified that spans 265 amino acids from position 365 to 629. It is composed of eight repeats of 33 amino acids each, not separated by spacers except for a single proline residue that separates three amino-terminal repeats from five carboxy-terminal ones (Figs. 6B,C, and 7C). This can enable amino- and carboxy-terminal repeats to function as individual blocks that can be rotated around the proline. Immediately downstream of ankyrin repeats lie two subsequent potential P-loop motifs, ALTTDGKT and GHSGSGKT, identified through the consensus sequence G[A]XXXXGKT[S] at positions 631–638 and 687–694, respectively (Fig. 6B). DAP kinase also carries multiple potential sites for post-translational modifications (see legend to Fig.6) and has neither transmembranal domain nor signal peptide (SAPS prediction; Brendel et al. 1992). Finally, it is noteworthy that the most carboxy-terminal 20 amino acids are extremely rich in serines.

Discussion

Programmed cell death can be triggered by external stimuli among which diffusible cytokines may play an important positive role. Rescue of genes that function along the pathways that link the membranal signals at the receptor level to the final execution of cell death may therefore be a promising approach in studing the molecular basis of cell death. We report here on the rescue of two novel genes whose expression was indispensable for executing IFN-γ-induced cell death in HeLa cells. The system displayed some characteristics typical of programmed cell death, such as condensation and segmentation of nuclear chromatin, membranal blebbing, budding off of cytoplasmic projections, and loss of microvilli. In contrast, another frequent characteristic, the internucleosomal DNA fragmentation, did not occur in these cells (H. Berissi and A. Kimchi, unpubl.), as reported previously in several other examples of programmed cell death that take place in the apparent absence of nuclease activation (Cohen et al. 1992; Ucker et al. 1992; Schwartz et al. 1993). The appearance of cell

Figure 7. DAP kinase sequence homologies to other serine/threonine kinases and alignment of the ankyrin repeats of this protein. (*A*) Protein kinase domain sequences of the DAP kinase are aligned with the corresponding domains of other calmodulin-dependent kinases. The kinase subdomain structure (numbered I-XI) and the region implicated in calmodulin recognition and binding (designated as calmodulin regulatory region) are indicated. The obligatory conserved amino acids within the kinase domain are labeled with asterisks. Numbers at *right* mark positions relative to the amino terminus of primary translational products of each kinase. The solid background indicates identical amino acids within the compared kinases. The stippled background indicates positions where the amino acids are not identical but similar. (nm-mlck) Nonmuscle myosin light chain kinase (chicken); (sm-mlck) smooth muscle myosin light chain kinase (rat); (camdk-alph, -beta, -gamm) calcium/calmodulin-dependent protein kinase II α-, β-, and γ-subunits, respectively; (mlck-dicdi) *Dictyostelium discoideum* (slime mold) myosin light chain kinase. (*B*) Alignment of kinase subdomains II and III of DAP kinase and the corresponding domains of different cell cycle-dependent kinases. (dm2) *Drosophila* CDC2 homolog; (pssalre) human serine/threonine kinase PSSALRE; (kpt2) human serine/threonine protein kinase PCTAIRE-2; (kin28) yeast (*Saccharomyces cerevisiae*) putative protein kinase; (mo15) *Xenopus* protein kinase related to cdc2 that is a negative regulator of meiotic maturation; (kkialre) human serine/threonine protein kinase KKIALRE. (*C*) Alignment of DAP kinase ankyrin repeats. The solid background indicates identical amino acids. A consensus sequence of the DAP kinase ankyrin repeats is shown at the *bottom*. The position of each individual repeat along the cDNA is illustrated in Fig. 6B. (ar1–8) Ankyrin repeats.

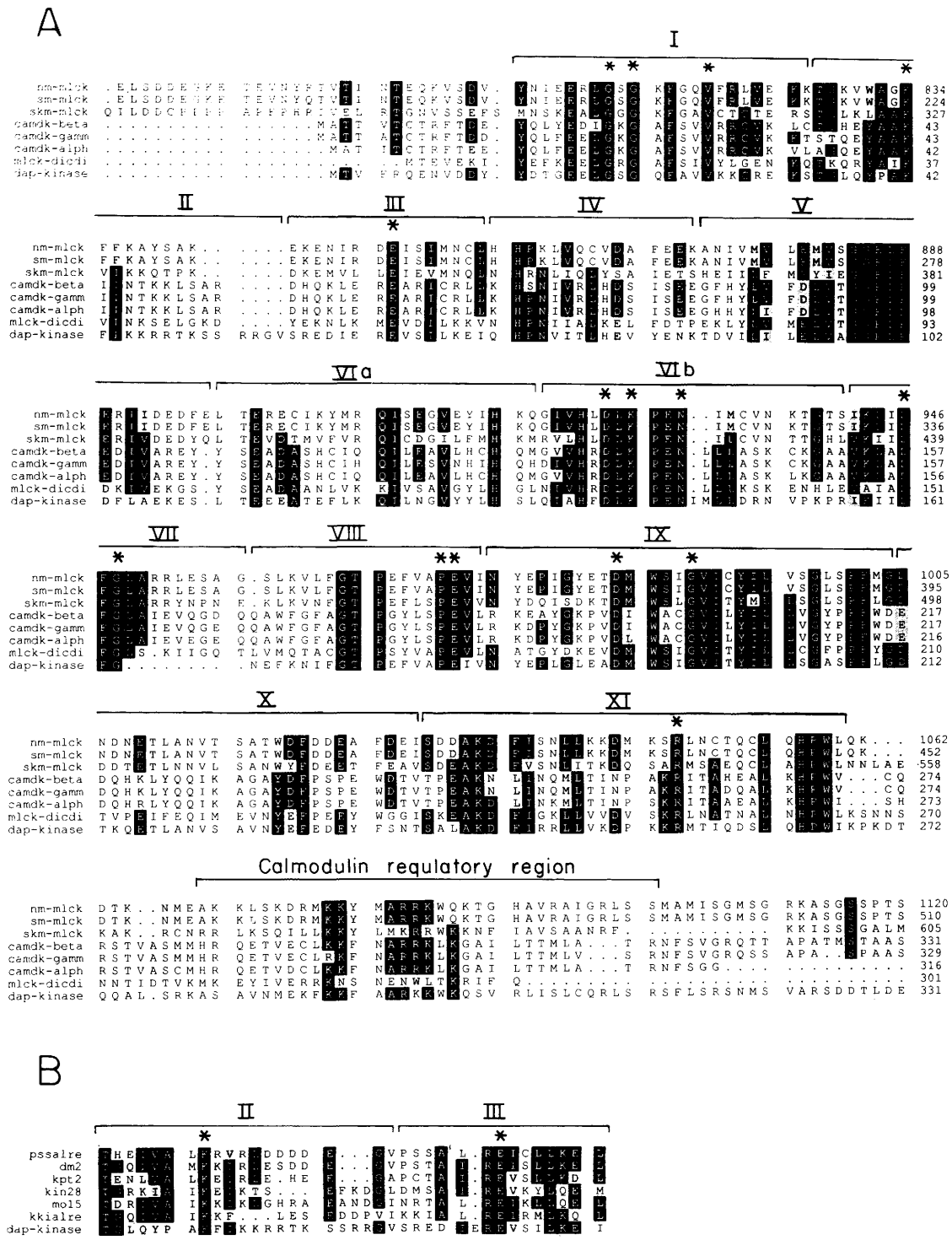

Figure 7. *(See facing page for legend.)*

death in this system could be accelerated very significantly by increasing the IFN-γ concentrations. The ability of IFN-γ to induce programmed cell death is consistent with previous reports that suggested a role for this cytokine in the negative selection by apoptosis of the peripheral T- and B-lymphocyte repertoire (Liu and Janeway 1990; Grawunder et al. 1993). IFN-γ has been long known as a cytokine causing the pathological type of cell death (termed necrosis) (Aune and Pogue 1989). So as with TNF-α (Laster et al. 1988), IFN-γ can induce either pathological or physiological cell death depending on the target cells.

So far, only a few genes (e.g., p53, c-*myc*, Ice, Ich-1) have been characterized as positive intracellular mediators of cell death in mammalian systems (Askew et al. 1991; Yonish-Rouach et al. 1991; Evan et al. 1992; Clarke et al. 1993; Lowe et al. 1993; Miura et al. 1993; Wang et al. 1994). One way to identify novel death-associated genes is to analyze the process in lower organisms, in which powerful genetic tools are available, as was initially done in the nematode *Caenorhabditis elegans*. Two positive modulators, *ced-3* and *ced-4*, were studied extensively in this system as well as a negative modulator of cell death, *ced-9*, that shares functional properties with the mammalian *bcl-2* gene (Ellis et al. 1991; Hengartner et al. 1992; Vaux et al. 1992; Yuan and Horvitz 1992; Yuan et al. 1993; Hengartner and Horvitz 1994). Another positive mediator of cell death was recently isolated from *Drosophila* (White et al. 1994). The identification of the mammalian homolog of *ced-3* as ICE, IL-1β-converting enzyme (Yuan et al. 1993), has lightened the importance of proteases in regulating cell death processes (Vaux et al. 1994).

In this work we suggest that functional selection of genes, by antisense RNA inactivation, can be used as a powerful approach for the rescue of positive mediators of cell death in mammalian cells. The two antisense cDNAs that were rescued here were capable of reducing the steady-state levels of the corresponding proteins in considerable amounts, thus slowing down the cell death process to an extent that enabled the positive selection. The mechanism by which the expression of the protein was reduced by the small antisense RNAs that have been selected by this method is still unknown. Yet, it is clear from our quantitations that a large excess of antisense versus sense RNA was required for both protein reduction and protection from IFN-γ-induced cell death. The HeLa/IFN-γ system that was employed in this work has the benefit of combining together the two major mechanisms that limit expansion in cell number, that is, proliferation arrest and cell death. This provides an opportunity to study the interrelationship between these different growth-restrictive processes and to find out whether they may share common genes as positive mediators. In this respect, it was found that the antiproliferative responses to IFN-γ were not interrupted by the inactivation of the two DAP genes, indicating that at some point growth arrest and programmed cell death pathways diverge and depend on different genes as positive mediators. It is also shown that the normal induction of the 2-5A synthetase gene, one of the IFN-induced immediate-early genes (Revel and Chebath 1986), was not interrupted (Fig. 2C). This finding indirectly excluded the possibility that the antisense RNAs may interfere with receptor-generated early signaling events that eventually transmit any of the biological effects of the cytokine. Also the reduction of c-*myc* mRNA expression that takes place several hours after exposure of HeLa cells to IFN-γ (Yarden and Kimchi 1986) was not interrupted by the antisense RNA (data not shown). The two DAP genes were found to be widely expressed as single transcripts in many cells and tissues (E. Feinstein and A. Kimchi, unpubl.). Therefore, it will be interesting to test whether the antisense RNA-mediated inactivation of these two genes may also interfere with programmed cell death, initiated by agents other than IFN-γ. It is already obvious from this work that a pathologic type of cell death induced in HeLa cells by TNF-α was refractory to the antisense mediated-inactivation of the two cloned DAP genes (Table 2).

The predicted amino acid sequence of DAP-1 and DAP kinase proteins showed no significant homology to known proteins; therefore, it is not possible at this stage to speculate about their function in cell death. The deduced amino acid sequence of the 15-kD DAP-1 predicts some interesting motifs and domains, yet their functional relevance still remains to be determined. The deduced amino acid sequence of the DAP kinase suggests that a very unique type of calmodulin-regulated serine/threonine kinase has been rescued. A combination of serine/threonine kinase domain, ankyrin repeats, and additional possible ATP/GTP-binding sites outside the kinase domain in one protein has not been described yet. A size of 160 kD is rare among serine/threonine kinases, and DAP kinase is actually the largest calmodulin-dependent kinase known to date. The ability of DAP kinase to bind calmodulin, confirmed in the yeast two-hybrid system (E. Feinstein and A. Kimchi, unpubl.), is consistent with the notion that in many cases programmed cell death is Ca^{2+} dependent (for review, see Sen 1992; Lee et al. 1993). Moreover, it has been reported recently that calmodulin antagonists inhibited the glucocorticoid-induced apoptosis, which implied that the activation of Ca^{2+}/calmodulin-dependent enzymes may mediate some types of cell death (Dowd et al. 1991). In another recent work it has been shown that inhibitors of myosin light chain kinases blocked the TNF-induced apoptotic cell death, a finding that may reflect the possible involvement of the DAP kinase in this system (Wright et al. 1993).

It is noteworthy that ankyrin repeats were not described before in the context of known serine/threonine kinases. One tyrosine kinase carrying ankyrin repeats has been identified recently in *Hydra vulgaris* (Chan et al. 1994). These 33 amino acid repeats, conserved from bacteria to man, were identified as important motifs involved in protein–protein interactions in a variety of proteins, including transmembranal proteins, transcription regulators, mitochondrial enzymes, and even extracellular toxins (Michaely and Bennett 1992). In the DAP ki-

nase, the eight ankyrin repeats could mediate the interaction with a putative effector or influence the substrate selectivity and/or stability of the kinase–substrate interactions. Two potential P-loop motifs were identified in DAP kinase outside the kinase domain, a feature not described in known kinases. Their comparison to the corresponding consensus sequences within seven ATP- or GTP-binding protein families (Saraste et al. 1990) demonstrates that only the 3′ sequence has some similarity to P-loop consensus of elongation factors, ATP synthase β-subunits, and thymidine kinase. Actually, a stretch of 33 amino acids following the eighth ankyrin repeat that encompasses the first putative P loop may represent a ninth ankyrin repeat that is less conserved than others. Additional work is clearly required to verify the true functional significance of this region.

Finally, it should be mentioned that death-controlling genes may be implicated in tumorigenesis upon gain of function (e.g., *bcl-2*) or loss of function (e.g., wild-type p53) mutations (Tsujimoto et al. 1985; Clarke et al. 1993; Lowe et al. 1993). Detailed chromosomal localization of the DAP genes and study of their expression in different human malignancies should be performed to test their possible involvement in tumorigenesis.

Materials and methods

Rescue of antisense cDNAs and secondary transfections

The construction of the HeLa cell cDNA library and its unidirectional cloning into the pTKO1 EBV-based episomal vector (downstream to the *Hin*dIII cloning site) was detailed previously (Deiss and Kimchi 1991). The cDNA library (100 μg of DNA) was introduced into 8×10^6 HeLa cells (10^6 cells/9-cm plate) by the standard calcium phosphate technique. The efficiency of stable transfections was 5%. After 48 hr the cultures were split and selected with both hygromycin B (200 μg/ml; Calbiochem) and IFN-γ (750 U/ml). Selective medium was changed every 3–4 days. After 28 days, pools of cells that remained on the plates were expanded for 15 days in medium containing only hygromycin, and the episomal DNA was extracted and cleaved with *Dpn*I restriction enzyme as detailed before (Deiss and Kimchi 1991). Plasmid DNA was isolated from 13 selected bacterial colonies. The cDNA inserts of groups 2 and 5 correspond to internal *Bam*HI–*Hin*dIII cDNA fragments generated because of incomplete methylation of cleavage sites during library construction. For secondary transfections subconfluent monolayers of HeLa cells were transfected with 40 μg of DNA of the individual rescued pTKO1 plasmids (in duplicates) and subjected to the single selection of hygromycin B. Pools of $\sim10^4$ hygromycin-resistant clones were generated from each transfection and were kept as stable polyclonal populations.

RNA and DNA blot analysis

Total RNA was extracted by the LiCl procedure as detailed previously (Einat et al. 1985) or by the guanidine/thiocyanate technique (Chomczynski and Saachi 1987). Samples of 20 μg of total RNA were fractionated on agarose gels, transferred to Hybond-N membranes (Amersham), and hybridized to DNA probes that were labeled with ^{32}P by the random primer labeling method using commercial kits (Boehringer). Prehybridization, hybridization, and washing of filters were carried out under stringent conditions as described previously (Yarden and Kimchi 1986). When indicated, the DNA probe was a PCR-amplified cDNA insert of the pTKO1 vector. It was generated by primers that correspond to the flanking sequences of the cDNA insertion sites within the vector. The oligonucleotides used were 5′-TCCAGAAGTAGTGAGGAGGC-3′ and 5′-TATGTCACACCACAGAAGTAAGG-3′.

Neutral red uptake assay and DAPI staining of DNA

The different transfected HeLa cell populations were cultivated in 96-well microtiter plates at an initial number of 15,000 cells/well for testing sensitivity to IFN-γ (750 U/ml or 5000 U/ml). Fresh meduim and drugs were supplemented every 3–4 days. When indicated, viable cells were stained with neutral red (Sigma) as detailed previously (Wallach 1984). The dye uptake was measured in quadruplicate at $\lambda = 540$ nm using an automated Micro-Elisa auto-reader. For testing the sensitivity to TNF-α, HeLa cell populations were seeded at an initial density of 30,000 cells per well. A mixture of TNF-α (200 U/ml) and CHX (25 μg/ml) was then added, and the cells were stained with neutral red at 5 and 20 hr after treatment. For DAPI staining, detached cells, collected from supernatants of IFN-γ-treated cultures (in 9-cm plates), were concentrated in 50 μl of phosphate-buffered saline, fixed with 50 μl of 3% paraformaldehyde, and cytospinned on glass slides. Cells were stained with DAPI (0.5 μg/ml; Sigma) for 10 min and mounted with Mowiol. Microscopy was perfomed under fluorescent light conditions.

Isolation of DAP-1 and DAP kinase cDNAs and nucleotide sequence analysis

The radioactively labeled cDNA inserts from pTKO1-230 and pTKO1-256 were used to screen two amplified λgt 10 cDNA libraries prepared from poly(A)$^+$ RNA of HL-60 and K562 cells, respectively. Approximately 4×10^5 PFU were screened with the 230 cDNA insert, and 10 positive clones were analyzed further by restriction enzyme mapping. About 4×10^6 PFU were screened with the 256 cDNA insert, and 40 positive clones were isolated after two rounds of sequential walking screening. Plaque hybridization was performed under stringent conditions. Two independent clones from each library, carrying the longest cDNA inserts, were chosen for further work. The four cDNA inserts were subcloned into Bluescript vectors. The sequencing was fully automatic and was performed on Applied Biosystems DNA sequencer 373 A.

Sequence uniqueness and relatedness was determined using FASTA (GCG software package) at the nucleotide level and FASTA, BLASTP, and BLOCKS programs at the amino acid level (Altschul et al. 1990; Henikoff et al. 1991).

Expression of DAP-1 in reticulocyte lysates and in bacterial systems

The cDNA inserts from λ1 cloned into Bluescript, as well as the subclones that were derived from them (p6, p5, p4, p8), were used as templates for in vitro transcription. RNA (0.5 μg) was then translated in reticulocyte lysates (Promega) using the conventional procedures, with [^{35}S]methionine as a labeled precursor. The in vitro-synthesized proteins were analyzed by fractionation on a 12% SDS–polyacrylamide gel followed by salicylic acid amplification of the radioactive signal. To mutate the ATG at position 160–162, oligonucleotide-directed mutagenesis was performed on subclone p6 (ATG was converted into GGC). For DAP-1 expression in bacteria, a *Nde*I site was generated in the p6 subclone at the first ATG (position 160–162) by

oligonucleotide-directed mutagenesis. After cleavage, the resulting *Nde*I–*Bam*HI 840-bp fragment was cloned into pET-3a bacterial expression vector and used to transform BL21 bacteria. A DAP-1-glutathione–*S*-transferase (GST) fusion construct was prepared by subcloning the 840-bp fragment in pGEX-2T; the fused protein was affinity purified on gluthatione–Sepharose beads (Pharmacia).

Preparation of anti-DAP-1 and DAP kinase antibodies and immunoblot analysis

Antibodies against GST–DAP-1-fused protein were prepared in rabbits. The sera were depleted of anti-GST antibodies by passing through CNBr-activated Sepharose beads (Pharmacia) coupled to GST and then were affinity purified on GST–DAP-1 cross-linked to Sepharose columns. Antibody titration was done with the 15-kD DAP-1 expressed from pET-3a in BL21 bacteria. Rabbit polyclonal antibodies, raised against the amino-terminal peptide (KTVFRQENVDDYYDTGEELG) of DAP kinase, were coupled via glutaraldehyde to tuberculin PPD (Statens Seruminstitute) and affinity purified on agarose–paranitrophenol column as described (Wilchek and Miron 1982). Cell lysates were prepared as described previously (Resnitzky and Kimchi 1991) for the DAP-1 analysis and in PLB buffer (10 mM phosphate buffer at pH 7.5; 100 mM NaCl; 1% Triton X-100; 0.5% sodium deoxycholate; 0.1% SDS; 5 mM EDTA) for DAP kinase detections. The COS-7 cells were transiently transfected with the PECE–FLAG expression vector that carries a fragment of the λ29 cDNA (from the start ATG, where the *Nde*I site was introduced by oligonucleotide-directed mutagenesis, to the first *Eco*RI site at the 3′ end; see Fig. 6A). Immunoblots were prepared as described previously (Resnitzky and Kimchi 1991) using the ECL Western blotting detection system. The specificity of signals was confirmed by competition with excess 15-kD bacterially expressed DAP-1 or excess of the DAP kinase amino-terminal peptide.

Immunoprecipitation and autophosphorylation of recombinant DAP kinase

Samples of cell lysates (400 μg) prepared before and after transfection of COS-7 cells with the PECE–FLAG–DAP kinase vector were immunoprecipitated with 2.9 μg of anti-FLAG M2 monoclonal antibodies (IBI) in 0.5 ml of IP buffer (50 mM Tris at pH 7.6, 5 mM EDTA, 150 mM NaCl, 0.1% Triton X-100, 0.1 mM $NaVO_3$, 10 mM NaPPi, 1 mM PMSF, 0.1 mM NaF, 100 μg/ml of leupeptin, 1.5 μg/ml of pepstatin A, 2 μg/ml of antipain, 4 μg/ml of aprotinin, 2 μg/ml of chymostatin). After 2 hr of incubation at 4°C, 20 μl of protein A+G coupled to agarose beads (Santa Cruz) was added for 1 hr. Immune complexes were washed twice with IP buffer and twice with the kinase assay buffer (50 mM HEPES at pH 7.5, 8 mM $MgCl_2$, 2 mM $MnCl_2$). The kinase assay was perfomed in 50 μl of kinase buffer supplemented with 0.1 mg/ml of BSA, 1 μM calmodulin, 0.5 mM $CaCl_2$, 50 μM ATP, 2 pmoles of [γ-^{32}P]ATP (5000 Ci/nmole, Amersham) for 20 min at 25°C. This was followed by two successive washes of the immune complexes with kinase buffer, followed by polyacrylamide gel fractionation.

Cytokines

Recombinant human IFN-γ was purified to 10^7 U/mg as detailed previously (Yarden and Kimchi 1986). Human recombinant TNF-α was kindly provided by Cetus Corporation and used in a final concentration of 20 ng/ml (which is equivalent to 200 U/ml).

Acknowledgments

We thank Drs. D. Reisman and V. Rotter for the gift of the HL-60 cDNA library, Dr. E. Canaani for the gift of the K562 cDNA library, Drs M. Rubinstein and D. Novick for human IFN-γ, and Cetus corporation for TNF-α. We thank Dr. H. Cahana for helpful discussions and Drs. J. Chebath and M. Revel for the 2-5A synthetase cDNA. The technical assistance of Dr E. Klein and Mrs. S. Gutman in the electron microscopy studies is deeply acknowledged. This work was supported by the German Cancer Research Center–Weizmann joint research program and Gesellschaft für Biotechnologische Forshung mbH. E.F. is Helena Rubinstein postdoctoral fellow in Biomedical Sciences and Cancer Research. The cDNA sequences were introduced into the nucleic acid data base; the accession numbers are X76104 and X76105 for DAP kinase and DAP-1, respectively.

The publication costs of this article were defrayed in part by payment of page charges. This article must therefore be hereby marked "advertisement" in accordance with 18 USC section 1734 solely to indicate this fact.

References

Altschul, S.F., W. Gish, W. Miller, E.W. Myers, and D.J. Lipman. 1990. Basic local alignment search tool. *J. Mol. Biol.* **215:** 403–410.

Askew, D.S., R.A. Ashmun, B.C. Simmons, and J.L. Cleveland. 1991. Constitutive c-myc expression in an IL-3-dependent myeloid cell line suppresses cell cycle arrest and accelerates apoptosis. *Oncogene* **6:** 1915–1922.

Aune, T.M. and S.L. Pogue. 1989. Inhibition of tumor cell growth by interferon-gamma is mediated by two distinct mechanisms dependent upon oxygen tension: Induction of tryptophan degradation and depletion of intracellular nicotinamide adenine dinucleotide. *J. Clin. Invest.* **84:** 863–875.

Blumenthal, D.K., K. Takio, A.M. Edelman, H. Charbonneau, K. Titani, K.A. Walsh, and E.D. Krebs. 1985. Identification of calmodulin-binding domain of skeletal muscle myosin light chain kinase. *Proc. Natl. Acad. Sci.* **82:** 3187–3191.

Brendel, V., P. Bucher, I.R. Nourbakhsh, B.E. Blaisdell, and S. Karlin. 1992. Methods and algorithms for statistical analysis of protein sequences. *Proc. Natl. Acad. Sci.* **89:** 2002–2006.

Chan, T.A., C.A. Chu, K.A. Rauen, M. Kroiher, S.M. Tatarewicz, and R.E. Steele. 1994. Identification of a gene encoding a novel protein-tyrosine kinase containing SH2 domains and ankyrin-like repeats. *Oncogene* **9:** 1253–1259.

Chomczynski, P. and N. Sacchi. 1987. Single-step method of RNA isolation by acid guanidinium thiocyanate-phenol-chloroform extraction. *Anal. Biochem.* **162:** 156–159.

Clarke, A.R., C.A. Purdie, D.J. Harrison, R.G. Morris, C.C. Bird, M.L. Hooper, and A.H. Wylie. 1993. Thymocyte apoptosis induced by p53-dependant and independent pathways. *Nature* **362:** 849–852.

Cohen, G.M., X.-M. Sun, R.T. Snowden, D. Dinsdale, and D.N. Skileter. 1992. Key morphological features of apoptosis may occur in the absence of internucleosomal DNA fragmentation. *Biochem. J.* **286:** 331–334.

Cowburn, D. 1994. Helical encounter. *Struct. Biol.* **1:** 489–491.

Cruzalegui, F.H., M.S. Kapiloff, J.-P. Morfin, B.E. Kemp, M.G. Rosenfeld, and A.R. Means. 1992. Regulation of intrasteric inhibition of the multifunctional calcium/calmodulin-dependent protein kinase. *Proc. Natl. Acad. Sci.* **89:** 12127–12131.

Deiss, L.P. and A. Kimchi. 1991. A genetic tool used to identify thioredoxin as a mediator of a growth inhibitory signal. *Science* **252:** 117–120.

Dowd, D.R., D.P. Mac, B.S. Komm, M.R. Haussler, and R. Miesfeld. 1991. Evidence for early induction of calmodulin gene expression in lymphocytes undergoing glucocorticoid-mediated apoptosis. *J. Biol. Chem.* **266:** 18423–18426.

Einat, M., D. Resnitzky, and A. Kimchi. 1985. Close link between reduction of c-myc expression by interferon and G0/G1 arrest. *Nature* **311:** 597–600.

Ellis, R.E., J.Y. Yuan, and H.R. Horvitz. 1991. Mechanisms and functions of cell death. *Annu. Rev. Cell. Biol.* **7:** 663–698.

Evan, G.I., A.H. Wyllie, C.S. Gilbert, T.D. Littlewood, H. Land, M. Brooks, C.M. Waters, L.Z. Penn, and D.C. Hancock. 1992. Induction of apoptosis in fibroblasts by c-myc protein. *Cell* **69:** 119–128.

Grawunder, U., F. Melchers, and A. Rolink. 1993. Interferon-γ arrests proliferation and causes apoptosis in stromal cell/interleukin-7 dependent normal murine pre-B cell lines and clones in vitro but does not induce differentiation to surface immunoglobulin-positive B cells. *Eur. J. Immunol.* **23:** 544–551.

Guerriero, V.J., M.A. Russo, N.J. Olson, J.A. Putkey, and A.R. Means. 1986. Domain organization of chicken gizzard myosin light chain kinase deduced from a cloned cDNA. *Biochemistry* **25:** 8372–8381.

Hanks, S.K. and A.M. Quinn. 1991. Protein kinase catalytic domain sequence database: Identification of conserved features of primary structure and classification of family members. Methods Enzymol. **200:** 38-62.

Hanks, S.K., A.M. Quinn, and T. Hunter. 1988. The protein kinase family: Conserved features and deduced phylogeny of the catalytic domains. *Science* **241:** 42–52.

Hengartner, M.O. and H.R. Horvitz. 1994. C. elegans cell survival gene ced-9 encodes a functional homolog of the mammalian proto-oncogene bcl-2. *Cell* **76:** 665–676.

Hengartner, M.O., R.E Ellis, and H.R. Horvitz. 1992. Caenorhabditis elegans gene ced-9 protects cells from programmed cell death. *Nature* **356:** 494-499.

Henikoff, S. and J.G. Henikoff. 1991. Automated assembly of protein blocks for database searching. *Nucleic Acids Res.* **19:** 6565–6572.

Herring, B.P., J.T. Stull, and P.J. Gallagher. 1990. Domain characterization of rabbit skeletal muscle myosin light chain kinase. *J. Biol. Chem.* **265:** 1724–1730.

Hofmann, S.L., J.L. Goldstein, K. Orth, C.R. Moomaw, C.A. Slaughter, and M.S. Brown. 1989. Molecular cloning of a histidine-rich Ca^{2+}-binding protein of sarcoplasmic reticulum that contains highly conserved repeated elements. *J. Biol. Chem.* **264:** 18083–18090.

Itoh, N., S. Yonehara, A. Ishii, M. Yonehara, S. Mizushima, M. Sameshima, A. Hase, Y. Seto, and S. Nagata. 1991. The polypeptide encoded by the cDNA for human cell surface antigen Fas can mediate apoptosis. *Cell* **66:** 233–243.

Kimchi, A. 1992. Cytokine triggered molecular pathways that control cell cycle arrest. *J. Cell. Biochem.* **50:** 1–9.

Laster, S.M., J.G. Wood, and L.R. Gooding. 1988. Tumor necrosis factor can induce both apoptic and necrotic forms of cell lysis. *J. Immunol.* **141:** 2629–2634.

Lee, S., S. Christakos, and M.B. Small. 1993. Apoptosis and signal transduction: Clues to molecular mechanism. *Curr. Opin. Cell. Biol.* **5:** 286–291.

Lin, J.K. and C.K. Chou. 1992. In vitro apoptosis in the human hepatoma cell line induced by transforming growth factor β1. *Cancer Res.* **52:** 385–388.

Liu, Y. and C.A. Janeway. 1990. Interferon-γ plays a role in induced cell death of effector T cell: A possible third mechanism of self-tolerance. *J. Exp. Med.* **172:** 1735–1739.

Lowe, S.W., E.M. Schmitt, S.W. Smith, B.A. Osborne, and T. Jacks. 1993. p53 is required for radiation-induced apoptosis in mouse thymocytes. *Nature* **362:** 847–849.

Michaely, P. and V. Bennett. 1992. The ANK repeat: A ubiquitous motif involved in macromolecular recognition. *Trends Cell Biol.* **2:** 127–129.

Miura, M., H. Zhu, R. Rotello, E.A. Hartwieg, and J. Yuan. 1993. Induction of apoptosis in fibroblasts by IL-1β converting enzyme, a mammalian homolog of the C. elegans cell death gene ced-3. *Cell* **75:** 653–660.

Oberhammer, F.A., M. Pavelka, S. Sharma, R. Tiefenbacher, A.F. Purchio, W. Bursch, and R. Schulte-Hermann. 1992. Induction of apoptosis in cultured hepatocytes and in regressing liver by TGF-β1. *Proc. Natl. Acad. Sci.* **89:** 5408–5412.

Olson, N.J., R.B. Pearson, D.S. Needleman, M.Y. Hurwitz, B.E. Kemp, and A.R. Means. 1990. Regulatory and structural motifs of chicken gizzard light chain kinase. *Proc. Natl. Acad. Sci.* **87:** 2284–2288.

Pongor, S., V. Skerl, M. Cserzo, Z. Hatsagi, G. Simon, and V. Bevilacqua. 1992. The SBASE domain library release: A collection of annotated protein sequence segments. *Nucleic Acids Res.* **21:** 3111–3115.

Resnitzky, D. and A. Kimchi. 1991. Deregulated c-*myc* expression abrogates the interferon and interleukin-6 mediated G0/G1 cell cycle arrest but not other inhibitory responses in M1 myeloblastic cells. *Cell Growth Differ.* **2:** 33–41.

Revel, M. and J. Chebath. 1986. Interferon-activated genes. *Trends Biochem. Sci.* **11:** 166–189.

Ruoslahti, E. and M.D. Pierschbacher. 1986. Arg-Gly-Asp: A versatile cell recognition signal. *Cell* **44:** 517–518.

Saraste, M., P.R. Sibbald, and A. Wittinghofer. 1990. The P-loop—A common motif in ATP- and GTP-binding proteins. *Trends Biochem. Sci.* **15:** 430–434.

Schwartz, L.M., S.W. Smith, M.E. Jones, and B.A. Osborne. 1993. Do all programmed cell deaths occur via apoptosis? *Proc. Natl. Acad. Sci.* **90:** 980–984.

Sen, S. 1992. Programmed cell death: Concept, mechanism and control. *Biol. Rev. Camb. Philos. Soc.* **67:** 287–319.

Shaw, G. and R. Kamen. 1986. A conserved AU sequence from the 3′ untranslated region of GM-CSF mRNA mediates selective mRNA degradation. *Cell* **46:** 659–667.

Shoemaker, M.O., W. Lau, R.L. Shattuck, A.P. Kwiatkowski, P.E. Matrisian, S.L. Guerra, E. Wilson, T.J. Lukas, E.L. Van, and D.M. Watterson. 1990. Use of DNA sequence and mutant analyses and antisense oligodeoxynucleotides to examine the molecular basis of nonmuscle myosin light chain kinase autoinhibition, calmodulin recognition, and activity. *J. Cell. Biol.* **111:** 1107–1125.

Smith, C.A., H.-J. Gruss, T. Davis, D. Anderson, T. Farrah, E. Baker, G.R. Sutherland, C.I. Brannan, N.G. Copeland, N.A. Jenkins, K.H. Grabstein, B. Gliniak, I.B. McAlister, W. Fanslow, M. Anderson, B. Falk, S. Gimpel, S. Gillis, W.S. Din, R.G. Goodwin, and R.J. Armitage. 1993. CD30 antigen, a marker for Hodgkin's lymphoma, is a receptor whose ligand defines an emerging family of cytokines with homology to TNF. *Cell* **73:** 1349–1360.

Suda,T., T. Takahashi, P. Golstein, and S. Nagata. 1993. Molecular cloning and expression of the Fas ligand, a novel member of the tumor necrosis factor family. *Cell* **75:** 1169–1178.

Trauth, B.C., C. Klas, A.M. Peters, S. Matzku, P. Moller, W. Falk, K.M. Debatin, and P.H. Krammer. 1989. Monoclonal antibody-mediated tumor regression by induction of apoptosis. *Science* **245:** 301–305.

Tsujimoto, Y., J. Cossman, E. Jaffe, and C.M. Croce. 1985. Involvement of bcl-2 in human follicular lymphoma. *Science* **228:** 1440–1443.

Ucker, D.S., P.S. Obermiller, W. Eckhart, J.P. Apgar, N.A.

Berger, and J. Meyers. 1992. Genome digestion is a dispensable consequence of physiological cell death mediated by cytotoxic T lymphocytes. *Mol. Cell. Biol.* **12:** 3060–3069.

Vaux, D.L., I.L. Weissman, and S.K. Kim. 1992. Prevention of programmed cell death in Caenorhabditis elegans by human bcl-2. *Science* **258:** 1955–1957.

Vaux, D.L., G. Haecker, and A. Strasser. 1994. An evolutionary perspective on apoptosis. *Cell* **76:** 777–779.

Wallach, D. 1984. Preparations of lymphotoxin induce resistance to their own cytotoxic effect. *J. Immunol.* **132:** 2464–2469.

Wang, L., M. Miura, L. Bergeron, H. Zhu, and J. Yuan. 1994. Ich-1, an Ice/ced-3-related gene, encodes both positive and negative regulators of programmed cell death. *Cell* **78:** 739–750.

White, K., M.E. Grether, J.M. Abrams, L. Young, K. Farrell, and H. Steller. 1994. Genetic control of programmed cell death in Drosophila. *Science* **264:** 677–683.

Wilchek, M. and T. Miron. 1982. *Biochem. Int.* **2:** 692–695.

Wright, S.C., H. Zheng J. Zhong, F.M. Torti, and J.W. Larrick. 1993. Role of protein phosphorylation in TNF-induced apoptosis: Phosphatase inhibitors synergize with TNF to activate DNA fragmentation in normal as well as TNF-resistant U937 variants. *J. Cell. Biochem.* **53:** 222–233.

Yarden, A. and A. Kimchi. 1986. Tumor necrosis factor reduces c-myc expression and cooperates with interferon-gamma in HeLa cells. *Science* **234:** 1419–1421.

Yonish-Rouach, E., D. Resnitzky, J. Lotem, L. Sachs, A. Kimchi, and M. Oren. 1991. Wild-type p53 induces apoptosis of myeloid leukaemic cells that is inhibited by interleukin-6. *Nature* **352:** 345–347.

Yuan, J. and H.R. Horvitz. 1992. The Caenorhabditis elegans cell death gene ced-4 encodes a novel protein and is expressed during the period of extensive programmed cell death. *Development* **116:** 309–320.

Yuan, J., S. Shaham, S. Ledoux, H.M.E. Ilis, and H.R. Horvitz. 1993. The C. elegans cell death gene ced-3 encodes a protein similar to mammalian interleukin-1β-converting enzyme. *Cell* **75:** 641–652.

Identification of a novel serine/threonine kinase and a novel 15-kD protein as potential mediators of the gamma interferon-induced cell death.

L P Deiss, E Feinstein, H Berissi, et al.

Genes Dev. 1995, **9:**
Access the most recent version at doi:10.1101/gad.9.1.15